Geomechanics and Engineering, *Vol. 12, No. 6 (2017) 965-981*
DOI: https://doi.org/10.12989/gae.2017.12.6.965

Influence of undercut and surface crack on the stability of a vertical escarpment

Sounik K. Banerjee [1a] and Debarghya Chakraborty [*2]

[1] *School of Civil Engineering, Kalinga Institute of Industrial Technology, Bhubaneswar, India*
[2] *Department of Civil Engineering, Indian Institute of Technology Kharagpur, Kharagpur, India*

(*Received April 20, 2016, Revised September 14, 2016, Accepted January 17, 2017*)

Abstract. Stability of vertical escarpments has been the subject of discussion for long time. However, available literature provides scarce knowledge about the effect of the formation of undercut and surface cracks on the stability of a vertical escarpment. The present study deals with a systematic analysis of the effect of surface cracks and undercut on slope stability using finite element based lower bound limit analysis. In the present analysis, the non-dimensional stability factor ($\gamma H/c$) is used to inspect the degrading effect of undercut and cracks developed at different offset distances from the edge of the vertical escarpment. Failure patterns are also studied in detail to understand the extent and the type of failure zone which may generate during the state of collapse.

Keywords: undercut; crack; vertical escarpment; lower bound limit analysis; failure

1. Introduction

Vertical slopes can be subjected to physical weathering from wind, water etc., which may result in the development of undercuts and tension cracks. These can drastically reduce the stability of vertical slopes. Historically, degradation of slope stability due to natural wear and tear has been dealt by numerous researchers. Deformations of a horizontally layered rock slope with partly exposed vertical joints was investigated by Tsesarsky *et al*. (2005) using a combination of finite element method and a technique namely discontinuous deformation analysis. Abderahman (2007) measured annual rate of undercutting of slopes with changes in sand content, porosity and identified their optimum values which controls the rate. Based on experimental study, Chu-Agor *et al*. (2008) concluded that the impact of turbulent river current on bank undercutting decreases its stability significantly. Zhang *et al*. (2012) reported case studies of slope failures due to human alterations, mainly because of the slope excavations for widening a highway. Michalowski (2012, 2013) investigated the impact of cracks on slope stability in the presence of seepage forces in the slope emphasizing the formation of a single large crack as one of the primary conditions of slope failure. Zhao (2015) provided the analytical solutions for horizontal crack propagation in a coal layer and underlying strata interface and also studied its effect on coal tunnel stability. Assuming rock slopes as a Mohr-Coulomb material, Miscevic and Vlastelica (2014) studied its strength

∗Corresponding author, Ph.D., E-mail: debarghya@civil.iitkgp.ernet.in
[a] M.Tech., E-mail: sbanerjee307@gmail.com

http://www.techno-press.org/?journal=gae&subpage=7 ISSN: 2005-307X (Print), 2092-6219 (Online)

reduction with weathering cycles. Regarding the available literature on the stability of vertical slope without any undercut and tension crack, Taylor (1937) provided stability charts using ϕ-circle method (an upper bound solution). By using the upper bound limit analysis technique, Chen *et al*. (1969) derived the slope stability charts. Bekaert (1995) used single and multiple rotation mechanisms (both upper bound in principle) to calculate the stability of slope. Florkiewicz and Kubzdela (2013) used statistical analysis to calculate slope safety factors. Michalowski (2002) presented slope stability charts using upper bound limit analysis in the presence of pore pressure. Yang and Pan (2015) and Gao *et al*. (2016) used upper bound limit analysis to assess the seismic stability of three dimensional steep slopes. Liu and Chen (2015) highlighted the strain localization in a slope using a strain softening material model. Hence, it is evident that the research on vertical slopes is quite common and well explored under different conditions with an exception of the effect of slope undercutting combined with vertical cracks resulting in a slope failure. The major contributions of this paper include (i) the estimation of reduction in stability of a vertical escarpment in presence of a horizontal undercuts; and (ii) the influence of vertical surface cracks on the stability of a vertical escarpment in the presence of undercuts. The present analysis is performed by using the lower bound finite element limit analysis with plain strain consideration. The stability of the vertical escarpment is expressed in terms of non-dimensional stability factor ($\gamma H/c$).

2. Problem definition

An undercut with a vertical depth of v (along y-axis) and a horizontal width of w (along x-axis) is present in a vertical escarpment of height (H) [refer Fig. 1(a)]. The change in the magnitude of stability factor ($\gamma H/c$) is required to be determined under the influence of different parameters, such as, the shape ratio of undercut (w/v), the crack depth ratio (d/v) and the offset ratio (f/v) for different magnitudes of H/v [refer Fig. 1(a)]. Stability charts are provided for cohesive-frictional materials. The Mohr-Coulomb yield criterion and an associated flow rule are assumed to be valid.

As the slopes generally collapse under self-load, the unit weight (γ) is maximized in the present optimization problem under a set of constraints discussed in the 'Analysis' section of the manuscript. The value of unknown γ is calculated for a certain value of cohesion (c) and height of the slope (H). However, representation of γ as $\gamma H/c$, a non-dimensional factor, helps in treating all the three variables in the expression as unknown design parameter while reading it from the chart. This way of expressing γ as $\gamma H/c$ can be found in various research papers using limit analysis involving a γ maximization technique. The presentation puts forward $\gamma H/c$ as a measure of slope stability and thus the percentage reductions refer to the negative effect of slope stability from the undercut and the surface cracks.

It should be noted that in reality, the shape of the undercut cannot be a perfect rectangle. Thus, the sides of the cut which may be slanting or rugged are simplified as a straight line for a particular value of w/v. In addition, irregular shapes create limitation to a proper study with parametric variations.

3. Mesh details and boundary conditions

A finite element mesh with three nodded triangular elements is used for the present study. The chosen domain and the stress boundary conditions are indicated in Fig. 1(a). Along the free

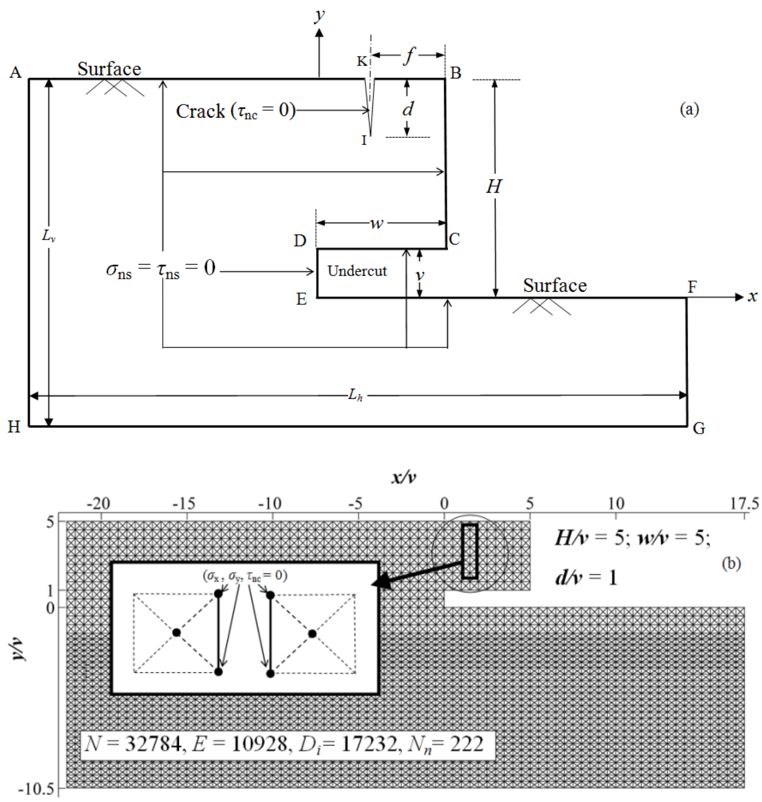

Fig. 1 (a) The schematic diagram of the problem with the appropriate boundary conditions; and (b) the finite element mesh with details developed for the analysis and mesh details exemplifying the numerical condition to introduce a vertical crack

boundaries (i.e., along AB, BC, CD, DE and EF) the normal stress (σ_{ns}) and shear stress (τ_{ns}) both are defined as zero (i.e., $\sigma_{ns} = \tau_{ns} = 0$). In addition, a vertical crack is introduced by using $\tau_{nc} = 0$ as another boundary condition along IK [refer Figs. 1(a) and 1(b)]. The size of the domain with vertical extent (L_v) and horizontal extent (L_h) are carefully chosen to eliminate the boundary effect on the results and save computation time. A typical finite element mesh used for the analysis with H/v = 5, d/v = 1, w/v = 5 and ϕ = 30° is presented in Fig. 1(b). This figure also provides specific values of different parameters, like N, E, D_i and N_c which refer to the total number of (i) nodes in the domain; (ii) elements in the domain; (iii) discontinuities in the domain; and (iv) nodes along the free surface of the domain, respectively.

4. Analysis

Following Lysmer (1970) and Sloan (1988), a finite element based lower bound formulation is used for the present study. Each node has three unknown stress variables, i.e., σ_x, σ_y and τ_{xy}. The unit weight (γ) of the in-situ material is considered as the objective function for linear optimization (as the only load resulting failure is the self-weight) and finally expressed as the non-dimensional stability factor ($\gamma H/c$) for usefulness. The unit weight is maximized subjected to a number of equality constraints satisfying (i) the equations of equilibrium; (ii) the continuity of the shear and normal stresses through adjacent elements; (iii) the stress boundary conditions, and also inequality constraints satisfying the linearized Mohr-Coulomb yield criterion (Bottero *et al.* 1980). For detailed numerical formulation one can refer to Chakraborty and Kumar (2013a).

Finally, after assembling all the equality and inequality constraints the expression for a linear optimization problem can be represented as follows

$$\text{Maximize:} \qquad \gamma \tag{1a}$$

$$\text{Subjected to:} \qquad [E_1]\{X\} = \{c_1\} \tag{1b}$$

$$[E_2]\{X\} \leq \{c_2\} \tag{1c}$$

where $[E_1]$ is the global matrix of equality constraints, $[E_2]$ is the global matrix of inequality constraint, $\{c_1\}$ is the global vector of equality constraint, and $\{c_2\}$ is the global vector of inequality constraint, and $\{X\}$ indicates a vector incorporating nodal unknown stresses and unit weight as

$$\{X\}^T_{(3N+1)} = \{\sigma_{x,1} \ \sigma_{y,1} \ \tau_{xy,1} \ \sigma_{x,2} \ \sigma_{y,2} \ \tau_{xy,2} \ \ldots\ldots \ \sigma_{x,N} \ \sigma_{y,N} \ \tau_{xy,N} \ \gamma\}$$

For carrying out the present analysis, a code is developed in MATLAB. The optimization is carried out by using LINPROG library function which is embedded in MATLAB.

5. Results and comparison

The variations of $\gamma H/c$ with w/v for different values of H/v and ϕ are presented in Fig. 2. This figure shows that the presence of an undercut in a vertical escarpment can reduce its stability substantially. Furthermore, the effect of a single vertical crack is introduced by using a parameter d/v (crack depth ratio) at a crack distance (f) from the face of the escarpment [side BC in Fig. 1(a)].

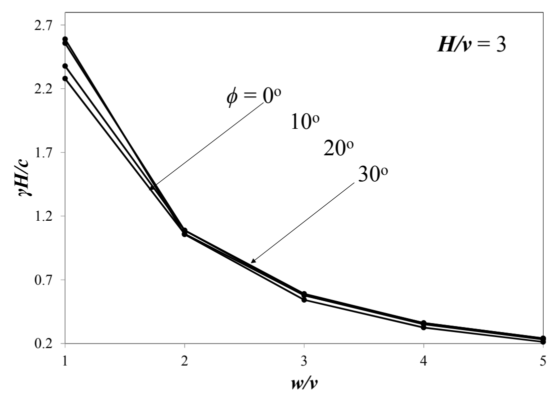

(a)

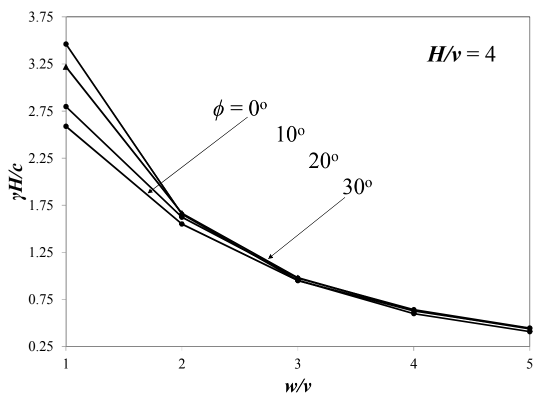

(b)

Fig. 2 The variation of stability factor ($\gamma H/c$) with w/v at different values of ϕ for (a) $H/v = 3$; (b) $H/v = 4$; (c) $H/v = 5$; (d) $H/v = 6$; (e) $H/v = 7$; and (f) $H/v = 8$

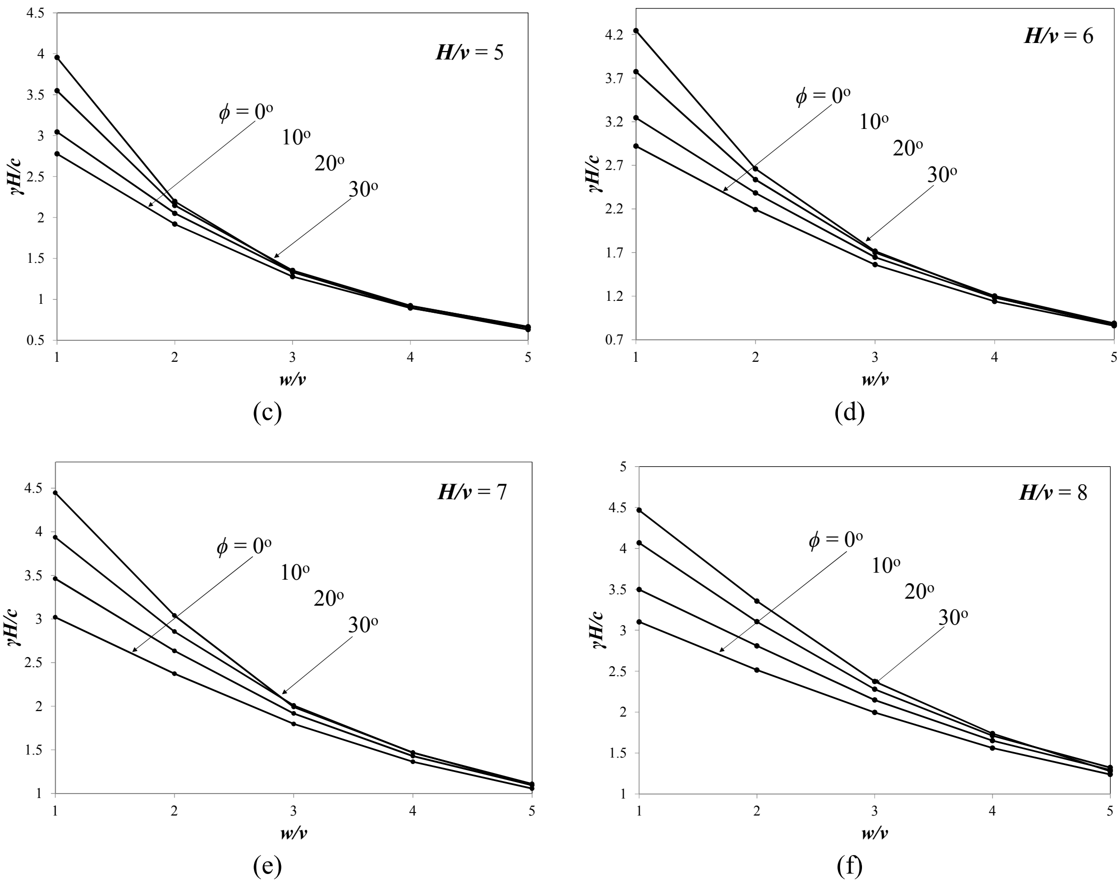

Fig. 2 Continued

For f/v = 1 with w/v = 1, 2 and 3 the effect of d/v (crack depth ratio) on the stability factor is presented in Figs. 3 and 4. Similarly, for f/v = 3 with w/v = 1, 2 and 3 the effect of d/v on the stability factor is presented in Figs. 5 and 6. In all the cases the friction angle of the in-situ material (ϕ) is varied in the range of 0°-30°.

It can be noted that for f/v = 1, the stability factor reduces remarkably for H/v = 3. However, for H/v = 7 this effect almost vanishes.

On the other hand, for f/v = 3 the stability factor is noted to remain almost unaffected for H/v = 3. However, as H/v increases to 5 and 7, the stability factor is found to reduce significantly. This aspect is elaborated in the failure pattern section making use of failure plots.

The effects of undercut (w/v) on the stability of vertical escarpment are illustrated in Fig. 7(a). The reduction factor (η), which is a ratio of the stability factor ($\gamma H/c$) with undercut to without undercut, is plotted along the y-axis with w/v along the x-axis. Noticeably, this ratio decreases with increase in ϕ for all H/v. It indicates higher rate of reduction in stability with increase in the friction angle. As expected, η increases with increase in H/v and decreases with increase in w/v. The minimum values of η (signifying the maximum reduction in stability) are observed at w/v = 5 for H/v = 3, 5 and 7 with ϕ = 0° as 0.064, 0.177 and 0.286 and with ϕ = 30° as 0.033, 0.100 and 0.174, respectively.

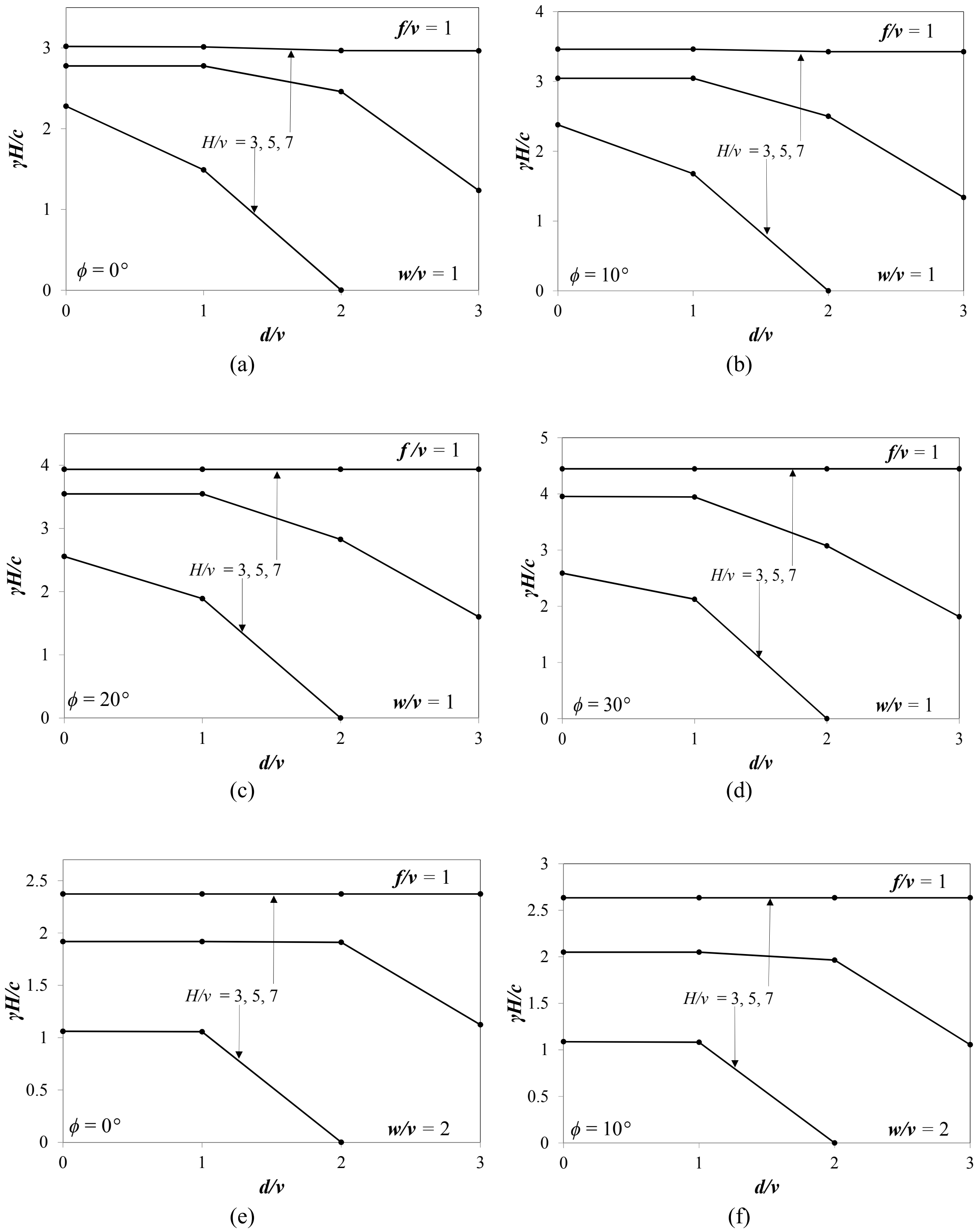

Fig. 3 The variation of stability factor ($\gamma H/c$) with d/v for different values of H/v when $f/v = 1$ for (a) $w/v = 1$, $\phi = 0°$; (b) $w/v = 1$, $\phi = 10°$; (c) $w/v = 1$, $\phi = 20°$; (d) $w/v = 1$, $\phi = 30°$; (e) $w/v = 2$, $\phi = 0°$; (f) $w/v = 2$, $\phi = 10°$; (g) $w/v = 2$, $\phi = 20°$; and (h) $w/v = 2$, $\phi = 30°$

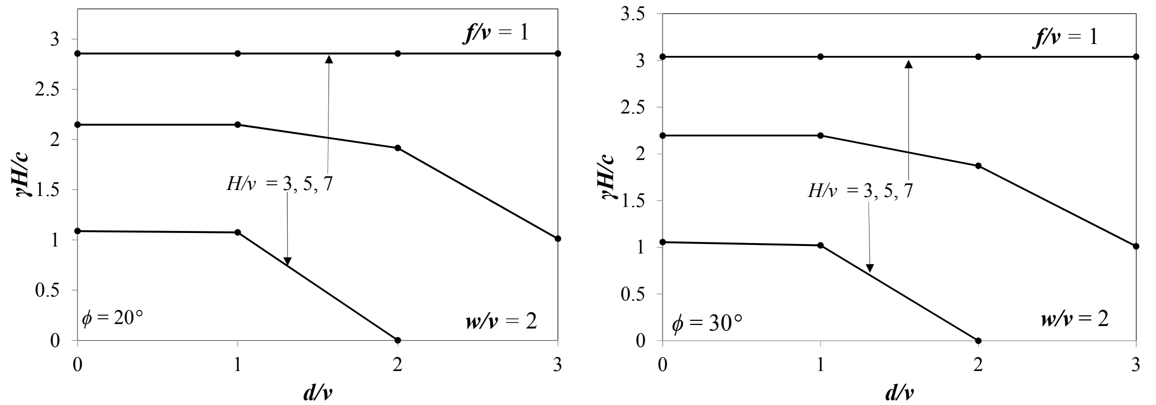

(g) (h)

Fig. 3 Continued

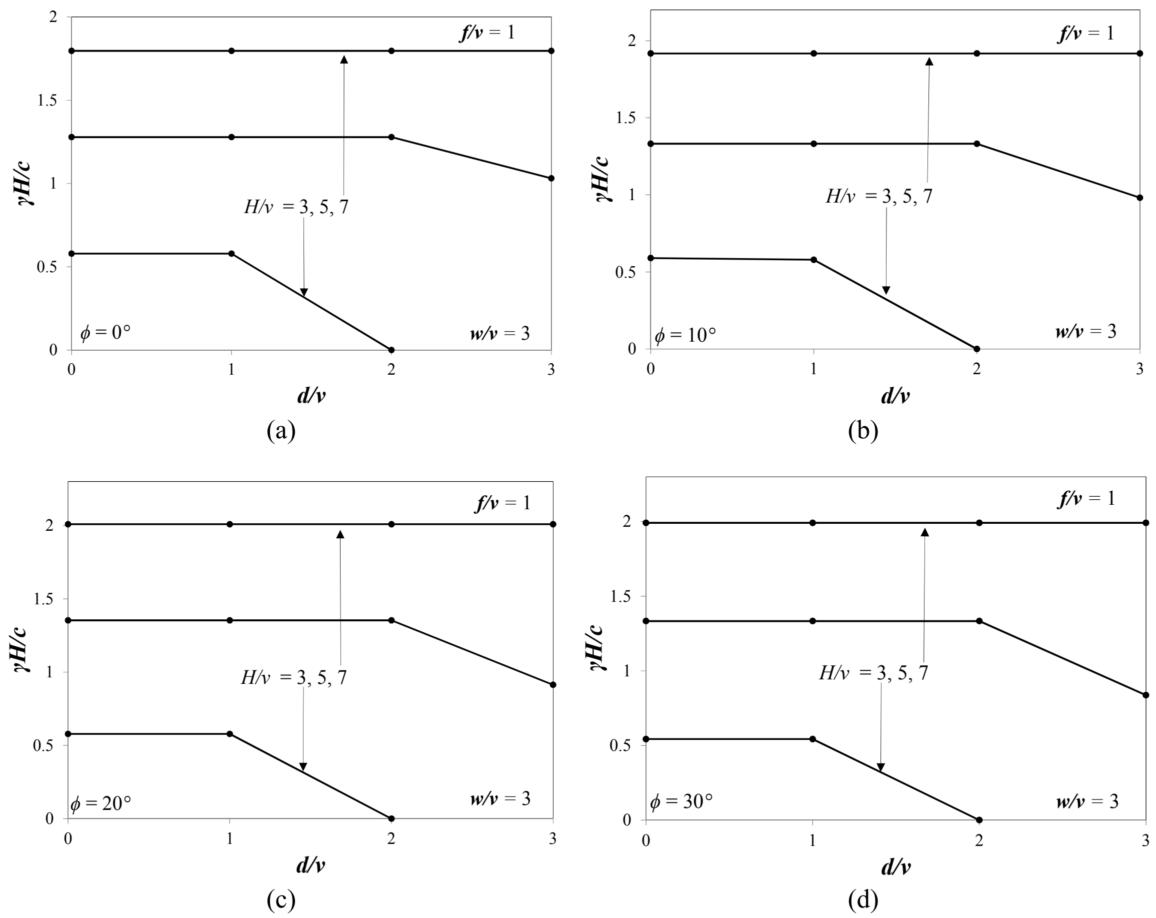

Fig. 4 The variation of stability factor ($\gamma H/c$) with d/v for different values of H/v when $f/v = 1$ for (a) $w/v = 3$, $\phi = 0°$; (b) $w/v = 3$, $\phi = 10°$; (c) $w/v = 3$, $\phi = 20°$; and (d) $w/v = 3$, $\phi = 30°$

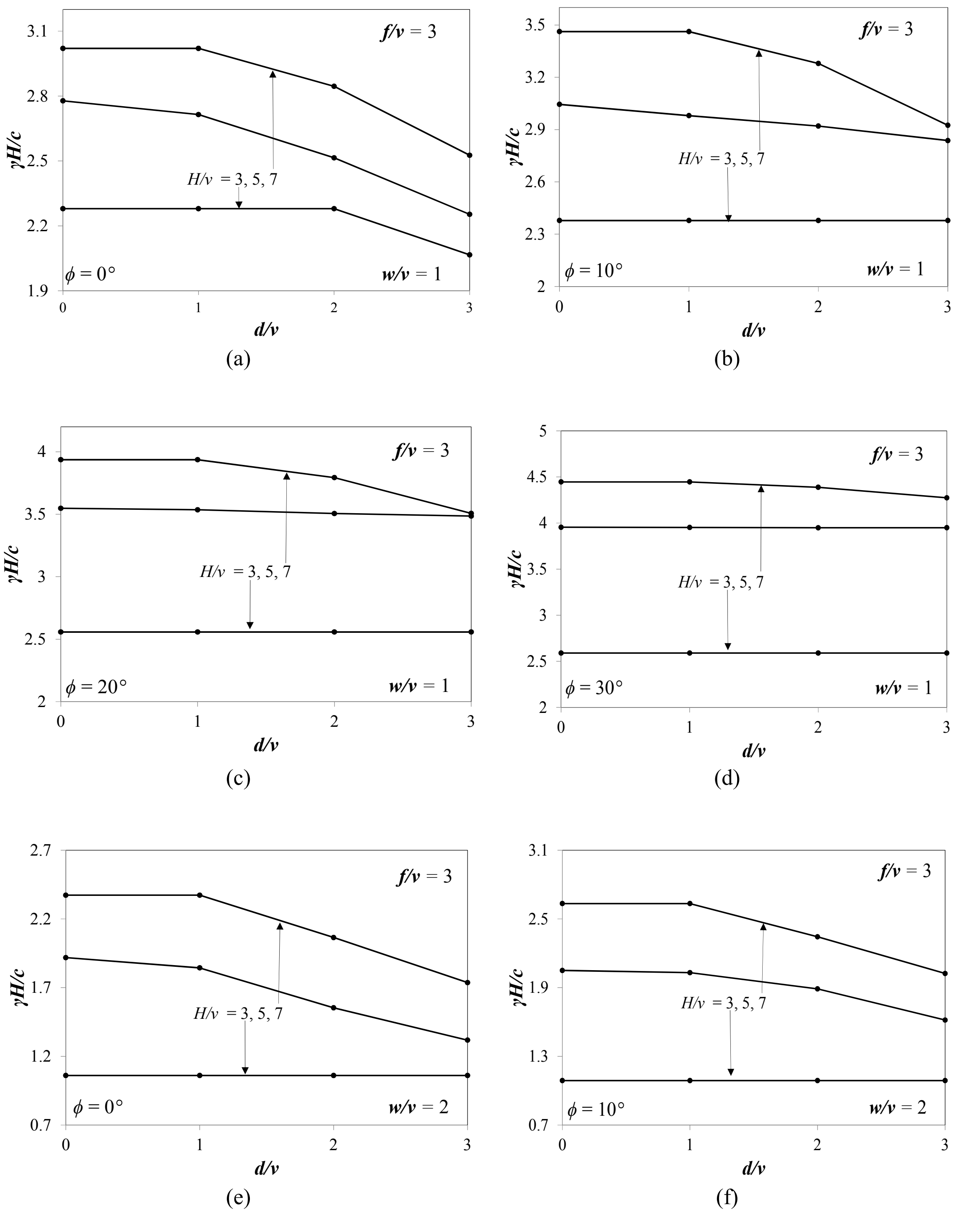

Fig. 5 The variation of stability factor ($\gamma H/c$) with d/v for different values of H/v when $f/v = 3$ for (a) $w/v = 1$, $\phi = 0°$; (b) $w/v = 1$, $\phi = 10°$; (c) $w/v = 1$, $\phi = 20°$; (d) $w/v = 1$, $\phi = 30°$; (e) $w/v = 2$, $\phi = 0°$; (f) $w/v = 2$, $\phi = 10°$; (g) $w/v = 2$, $\phi = 20°$; and (h) $w/v = 2$, $\phi = 30°$

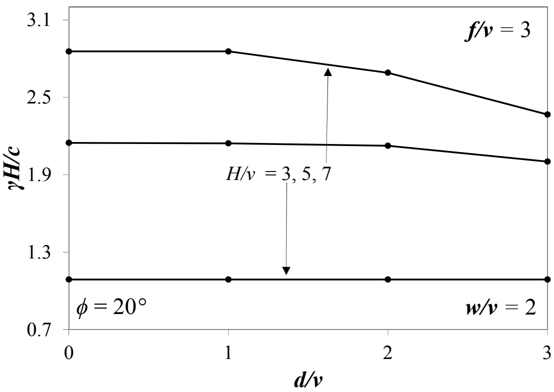

(g)

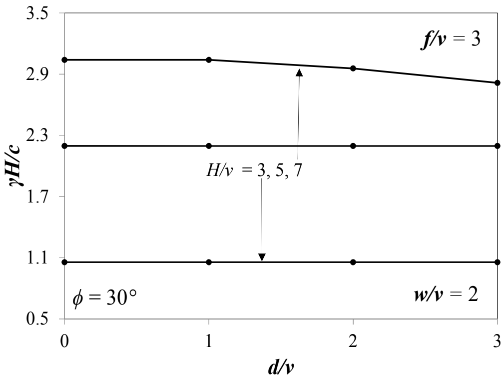

(h)

Fig. 5 Continued

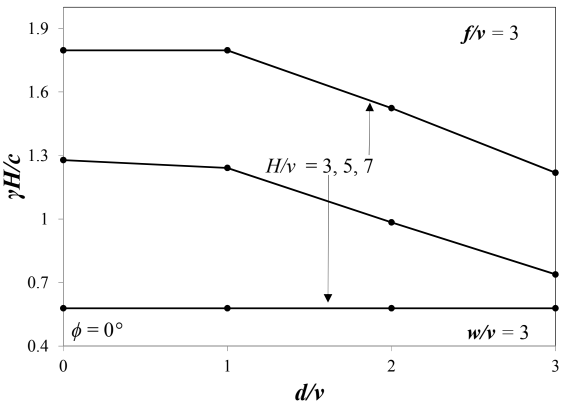

(a)

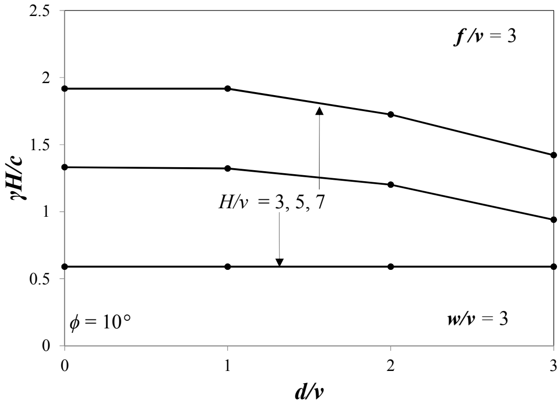

(b)

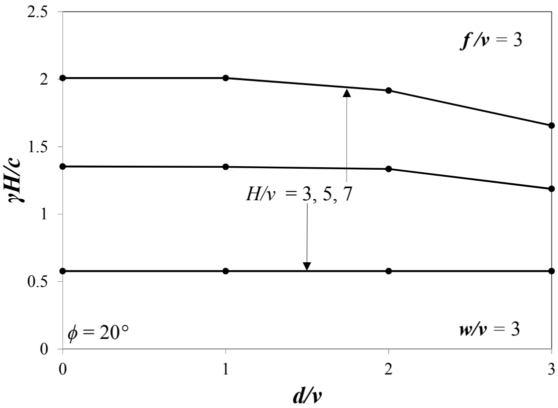

(c)

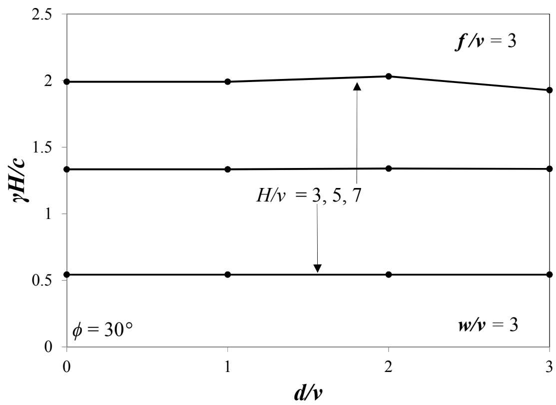

(d)

Fig. 6 The variation of stability number ($\gamma H/c$) with d/v for different values of H/v when f/v = 3 for (a) w/v = 3, ϕ = 0°; (b) w/v = 3, ϕ = 10°; (c) w/v = 3, ϕ = 20°; and (d) w/v = 3, ϕ = 30°

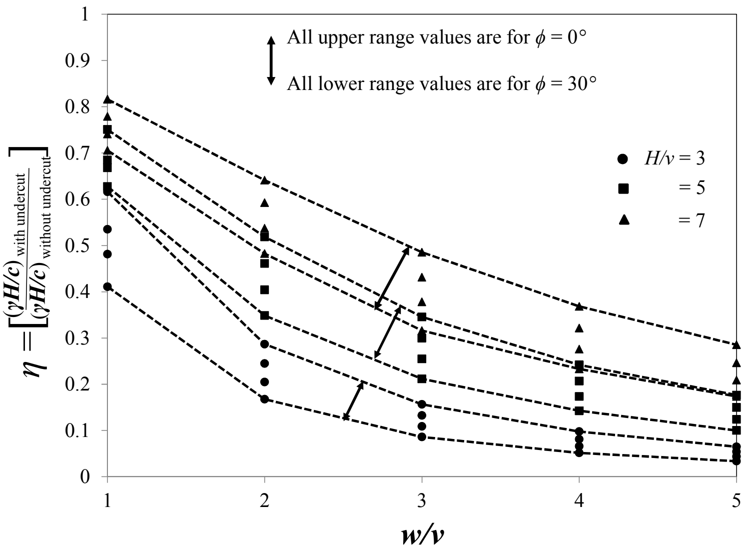

(a)

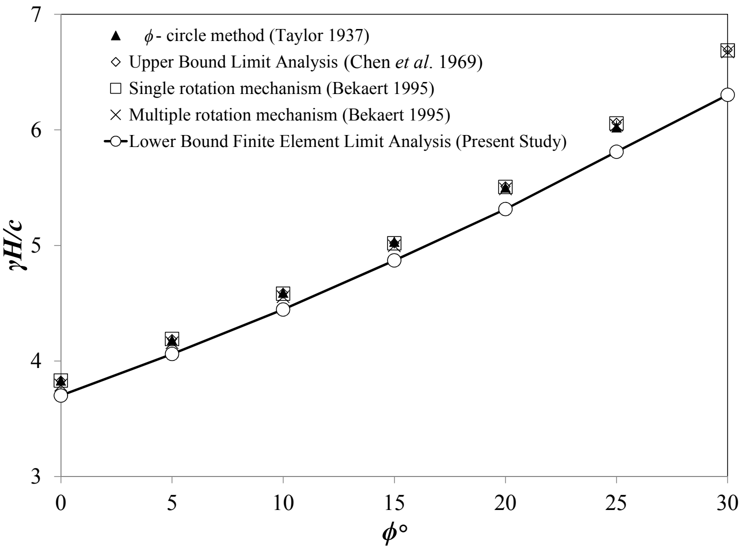

(b)

Fig. 7 (a) The variation of η with w/v for different values of ϕ and H/v; and (b) comparison of the present lower bound results with the available literature without any undercut and crack

As stability calculations of a vertical escarpment with undercuts and surface cracks are unavailable in literature, the same calculations for the escarpment are done without these weathering effects. These results calculated by using the lower bound limit analyses are subsequently compared with widely popular results available in literature (Taylor 1937, Chen *et al.* 1969, Bekaert 1995). The comparison is presented in Fig. 7(b). A good agreement is noted between the present lower bound results and the results available in literature.

6. Proximity of the stress state at a point with respect to the yield

The proximity of the stress state at a point with respect to the yield can provide an idea about the nature and the extent of high stress zones close to the failure condition. This is determined in terms of a ratio, a/d, where $a = (\sigma_x - \sigma_y)^2 + (2\tau_{xy})^2$ and $d = \{2c \cos\phi - (\sigma_x + \sigma_y) \sin\phi\}^2$. The magnitude of a/d can vary between 0 and 1. For a point at the yield state of stress, the value of a/d

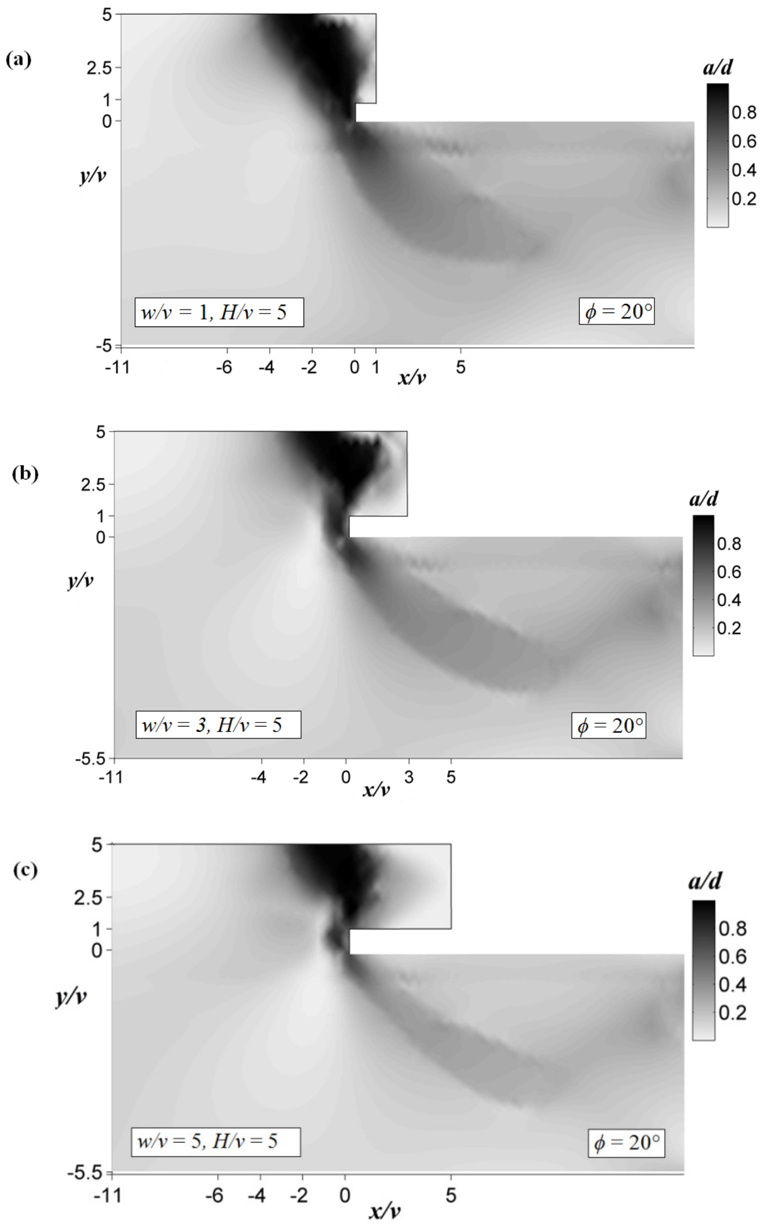

Fig. 8 Proximity to yield state plots observed for a vertical slope with undercut at $H/v = 5$, $d/v = 0$ and $\phi = 20°$ for (a) $w/v = 1$; (b) $w/v = 3$; and (c) $w/v = 5$

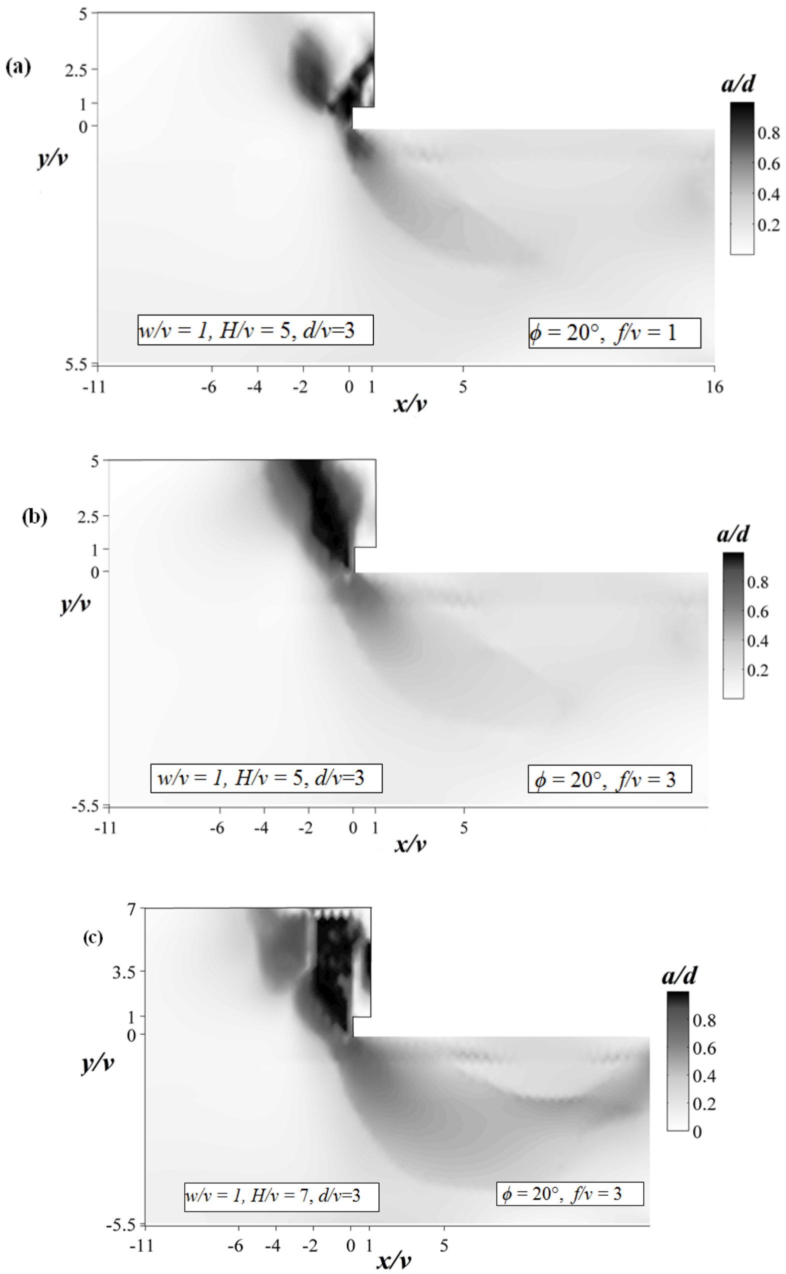

Fig. 9 Proximity to yield state plots observed for a vertical slope affected by crack offset ratio (f/v) with $\phi = 20°$, $w/v = 1$, $d/v = 3$ for (a) $H/v = 5$, $f/v = 1$; (b) $H/v = 5$, $f/v = 3$; and (c) $H/v = 7$, $f/v = 3$

becomes simply equal to unity. On the other hand, for non-yielding points, the value of a/d will remain smaller than 1. The proximity of the stress state to the yield plots of a vertical escarpment for different values of w/v at $H/v = 5$, $\phi = 20°$ and $f/v = 0$ (no crack), are presented through Figs. 8(a)-(c). While Figs. 9(a) and (b) show the effect of crack offset ratio f/v on the failure patterns at

$H/v = 5$, $\phi = 20°$ and $d/v = 3$. Fig. 9(c) shows the same effect for $H/v = 7$.

It can be clearly observed that as the size of the undercut increases ($w/v = 1$ to 5), the failure zone widens near the top surface of the vertical slope and shrinking towards its base [see Figs. 8(a)-8(c)]. Also, it shifts away from the vertical face [towards BC in Fig. 1(a)]. The zone of failure can also be observed to be reducing from about $7D$ to $5D$ along the x-axis for an increase in w/v from 1 to 5.

Fig. 9(a) shows a small spread of the black area or a local zone very close to failure or yielding. This represents a situation when the crack is relatively close to the vertical wall of the escarpment ($f/v = 1$). At this relative position of the crack, the close to yielded zone changes into a wider, conventional slope failure when $H/v = 7$ (not shown in the contour plot). This can be understood from the less affected values of $\gamma H/c$ for higher H/v in Figs. 3 and 4. This widening of the failure zone can also be observed as the crack moves away from the wall ($f/v = 3$) [see Figs. 9(b) and 9(c)]. This is governed by the self-weight of the material. The splayed yielded zone signifies the degrading influence of a crack on the slope stability. Also as expected, the effect of the crack on the stability can be seen to increase with H/v (from 5 to 7) [see Figs. 9(b) and 9(c)]. This fact is further supported by Figs. 6(a)-6(d) for a larger crack depth of $d/v = 3$.

It should be clearly mentioned here that though the light dark areas ($a/d < 1$ or non-plastic areas) in Figs. 8(b), 8(c) and 9(c) extend to the domain boundary on the right, it does not in any way affect the stability factor values; i.e., increasing the domain extent does not resulted in change in $\gamma H/c$.

Note that the present analysis is erected on a mesh density which if altered with an increase or decrease, negligibly affects the results. Hence, the failure patterns developed is also consistent and is unlikely to vary with mesh variation.

7. Few comments and explanations on various aspects of the present problem are point-wise discussed in this section

- It should be mentioned here that the stability factor considered in this problem is same as the standard stability factor. However, the Taylor's stability number is the reciprocal of this factor.
- The effort is made to find out the effect of the parameters representing the undercut in non-dimensional form. The case of a slope without an undercut can be indicated by an undercut of zero thickness ($w = 0$), resulting in $w/v = 0$. This means, as we assume a height of an undercut hypothetically, its width of zero clearly suggests the absence of it.
- Note that in reality the shape of the undercut may be irregular; however, for simplicity and also for carrying out a suitable parametric study, the undercut considered in the present problem is generalized as rectangular in shape. It should be mentioned here that in case of an undercut of irregular shape the effect may be approximately dealt with by considering an equivalent cross-sectional area ($w \times v$) for a particular w/v ratio; where w and v are the approximate width and depth of the undercut of irregular shape, respectively. As w and v are presented as a ratio, both can be variables. For illustration, at $w/v = 2$, w can attain value 1, 2, 3, 4 and v will take 0.5, 1, 2/3 and 2, respectively.
- The cracks in the surface of a vertical slope may develop as a result of slope failure from undercutting. Also, it is quite possible that weathering agents like freeze and thaw may also result in the vertical cracks which then pose instability to the slope as a separate cause and

not as a coupled effect of undercutting. The second case is considered in the present problem.

- It should be mentioned that the quantitative conclusions are made after observing the global trend over the ranges of the various parameters like H/v, w/v and f/v. For example, the values of $\gamma H/c$ for a vertical slope without undercut and vertical crack ($H/v = \infty$, $w/v = 0$, $f/v = 0$) are 3.70, 4.45, 5.31 for $\phi = 0°$, 10° and 20°, respectively (refer the present results obtained from Fig. 7b). Whereas, $\gamma H/c$ results obtained for $H/v = 7$, $w/v = 1$, $f/v = 0$ are 3.02, 3.46 and 3.94 for $\phi = 0°$, 10° and 20°, respectively (refer Fig. 2(e)). This reduction in $\gamma H/c$ can be presented as a percentage reduction of 18.38%, 22.25% and 25.8%, respectively.
- It should be noted that the soil heterogeneity conditions like layered soils, inclusion of geotextiles, directional anisotropy can be modeled using the bound theorems of finite element based limit analysis. For example, to model a layered soil as a Mohr-Coulomb material, the nodes in different layers are assigned different c-ϕ values representing their variation in properties. In the same fashion, a soil in which the cohesion increases with depth can be modeled (Davis and Booker 1973, Sloan 1988, Sloan and Kleeman 1995). Inclusion of geotextiles can be modeled by using the proposed formulation of Chakraborty and Kumar (2013b).
- In the current work, heterogeneity is not directly introduced; however, following the conversion chart for heterogeneous soils by Poulos and Davis (1980), heterogeneity condition can be addressed by the present problem.

8. Conclusions

In the present problem, the vertical soil slope is assumed to be unsupported. Therefore, the use of retaining walls, bracings or ground improvement techniques like soil nailing, soil grouting etc. will only increase the escarpment stability. In general, evaluating the effects of an undercut at the base of a vertical slope and a vertical crack which propagates vertically from its surface, the following conclusions can be drawn:

- The creation of an undercut significantly reduces the stability of a vertical escarpment with a maximum reduction of 96.7% at $H/v = 3$ and 82.6% at $H/v = 7$ within the boundaries of the present data analysis.
- The reduction in slope stability due to the presence of undercut is found to have a higher impact with increase in the friction angle of the in-situ material.
- Presence of vertically propagating cracks close to the face of the vertical escarpment results in localized failures. For $f/v = 1$; the crack depth ratio (d/v) of 2 has recessed the escarpment stability by 100% compared to the same at $d/v = 0$, irrespective of the change in the shape ratio of undercut (w/v).
- Cracks formed with higher offset (f/v) tend to affect stability of higher (H/v) slopes than smaller ones.

Finally, it is expected that the charts provided in this paper will be useful for the practicing engineers to predict the loss of a slope when the material strength is expressed in terms of c and ϕ. The effect of undercut and cracks caused by weathering on slope stability can be captured from the charts. This can provide a good understanding on the health of a slope while monitoring these weathering parameters. Thus it can help in a better management of a slope failure by comparing the field $\gamma H/c$ (measuring the height of the slope H, in-situ γ and in-situ c) with the presented values.

References

Abderahman, P. (2007), "Evaluating the influence of rate of undercutting on the stability of slopes", *Bull. Eng. Geol. Environ.*, **66**(3), 303-309.
Bekaert, P. (1995), "Improvement of the kinematic bound for the stability of a vertical cut-off", *Mech. Res. Commun.*, **22**(6), 533-540.
Bottero, A., Negre, R., Pastor, J. and Turgeman, S. (1980), "Finite element method and limit analysis theory for soil mechanics problem", *Comput. Method. Appl. Mech. Eng.*, **22**(1), 131-149.
Chakraborty, D. and Kumar, J. (2013a), "Stability of a long unsupported circular tunnel in soils with seismic forces", *Natural Hazards*, **68**(2), 419-431.
Chakraborty, D. and Kumar, J. (2013b), "Bearing capacity of circular footings on reinforced soils", *Int. J. Geomech.*, *ASCE*, **15**(1), 1-9.
Chen, W.F., Giger, M.W. and Fang, H.Y. (1969), "On the limit analysis of stability of slopes", *Soils Found.*, **9**(4), 23-32.
Chu-Agor, M.L., Wilson, G.V. and Fox, G.A. (2014), "Numerical modeling of bank instability by seepage erosion undercutting of layered stream-banks", *J. Hydrol. Eng.*, *ASCE*, **13**(12), 1133-1145.
Davis, E.H. and Booker, J.R. (1973), "The effect of increasing strength with depth on the bearing capacity of clays", *Géotechnique*, **23**(4), 551-563.
Florkiewicz, A. and Kubzdela, A. (2013), "Factor of safety in limit analysis of slopes", *Geomech. Eng.*, *Int. J.*, **5**(5), 485-497.
Gao, Y., Wu, D., Zhang, F., Lei, G.H., Qin, H. and Qiu, Y. (2016), "Limit analysis of 3D rock slope stability with non-linear failure criterion", *Geomech. Eng.*, *Int. J.*, **10**(1), 59-76.
Liu, D. and Chen, X. (2015), "Shearing characteristics of slip zone soils and strain localization analysis of a landslide", *Geomech. Eng.*, *Int. J.*, **8**(1), 33-52.
Lysmer, J. (1970), "Limit analysis of plane problems in soil mechanics", *J. Soil Mech. Found. Div.*, *ASCE*, **96**(4), 1311-1333.
Michalowski, R.L. (2002), "Stability charts for uniform slopes", *J. Geotech. Geoenviron. Eng.*, *ASCE*, **128**(4), 351-355.
Michalowski, R.L. (2012), "Stability assessment of slopes with cracks", *Proceedings of Geo-Congress*, Oakland, CA, USA, March, pp. 442-450.
Michalowski, R.L. (2013), "Stability assessment of slopes with cracks using limit analysis", *Can. Geotech. J.*, **50**(10), 1011-1021.
Miscevic, A. and Vlastelica, G. (2014), "Impact of weathering on slope stability in soft rock mass", *J. Rock Mech. Geotech. Eng.*, **6**(3), 240-250.
Poulos, H.G. and Davis, E.H. (1980), *Pile Foundation Analysis and Design*, Wiley, NewYork, NY, USA.
Sloan, S.W. (1988), "Lower bound limit analysis using finite-elements and linear programming", *Int. J. Numer. Anal. Method. Geomech.*, **12**(1), 61-77.
Sloan, S.W. and Kleeman, P.W. (1995), "Upper bound limit analysis with discontinuous velocity fields", *Comput. Method. Appl. Mech. Eng.*, **127**(1-4), 293-314.
Taylor, D.W. (1937), "Stability of earth slopes", *J. Boston Soc. Civil Eng.*, **24**(3), 197-246.
Tsesarsky, M., Hatzor, Y.H., Leviathan, I., Saltzman, U. and Sokolowksy, M. (2005), "Structural control on the stability of overhanging, discontinuous rock slopes", *Am. Rock Mech. Assoc.*, **5**, 771-781.
Yang, X.L. and Pan, Q.J. (2015), "Three dimensional seismic and static stability of rock slopes", *Geomech. Eng.*, *Int. J.*, **8**(1), 97-111.
Zhang, F., Liu, G., Chen, W., Liang, S., Chen, R. and Han, W. (2012), "Human-induced landslide on a high cut slope: a case of repeated failures due to multi-excavation", *J. Rock Mech. Geotech. Eng.*, **4**(4), 367-374.

Zhao, C. (2015), "Analytical solutions for crack initiation on floor-strata interface during mining", *Geomech. Eng., Int. J.*, **8**(2), 237-255.

CC

Nomenclature

E_1 = global matrix of equality constraint defined in Eq. 1(b)

E_2 = global matrix of inequality constraint defined in Eq. 1(c)

c_1 = is the global vector defined in Eq. 1(b)

c_2 = is the global vector defined in Eq. 1(c)

c = cohesion of the material

d = depth of the vertical crack

v = depth of the undercut along y-axis

w = width of the undercut along x-axis

E = total number of elements in domain

H = height of the vertical escarpment

f = offset distance of the crack from the edge of escarpment

L_v = vertical extent of material domain considered

L_h = horizontal extent of material domain considered

N = total number of nodes in domain

N_c = total number of nodes along free surface of the domain where normal and shear stresses are zero

X = global vector containing all unknown nodal stress and unit weight of the in-situ material

ϕ = angle of internal friction of the in-situ material

γ = unit weight of the material

σ_{ns} = normal stress component along AB, BC, CD, DE and EF

σ_x = normal stress component along x-axis

σ_y = normal stress component along y-axis

τ_{nc} = shear stress component along IK

τ_{ns} = shear stress component along AB, BC, CD, DE and EF

τ_{xy} = shear stress component in x-y plane